M&C 2017 - International Conference on Mathematics & Computational Methods Applied to Nuclear Science & Engineering, Jeju, Korea, April 16-20, 2017, on USB (2017)

Recent Progresses of Research on Sensitivity and Uncertainty Analysis for Reactor-Physics Calculation at XJTU

Liangzhi Cao, Hongchun Wu, Chenghui Wan, Yong Liu, Chao Yang, Wei Shen

Xi'an Jiaotong University, No. 28 Xianning West Road, Xi'an, Shaanxi Province, 710049, caolz@mail.xjtu.edu.cn

Abstract – *In this paper, the recent progresses of the researches on the sensitivity and uncertainty analysis for the reactor-physics calculations at XJTU have been presented. The widely applied deterministic method and statistical sampling method have been utilized and corresponding code programs have been developed. With the deterministic method, the Generalized Perturbation Theory (GPT) has been applied to perform the sensitivity and uncertainty analysis for the lattice calculations and burnup calculations, and corresponding home-developed codes named as NECP-COLEUS and NECP-SUNDEW respectively. For NECP-COLEUS, GPT is used to quantify the relative sensitivity coefficients of the important responses, including the eigenvalue and the few-group constants of the lattice calculations with respect to the cross sections; For NECP-SUNDEW, GPT is used to quantify the relative sensitivity coefficients of the important responses, including the eigenvalues and atomic densities with depletions of the burnup calculations to the cross sections. With the relative sensitivity coefficients of the important responses, both NECP-COLEUS and NECP-SUNDEW can quantify the uncertainties of corresponding responses introduced by the nuclear-data uncertainties. With the statistical sampling method (SSM), the code named NECP-UNICORN has been developed, and has the uncertainty-analysis capability for the lattice calculations and core simulations with depletions based on the "two-step" scheme for the reactor-physics calculations. For NECP-UNICORN, the uncertainties of the eigenvalues, kinetic parameters, few-group constants and atomic densities with depletions for the lattice calculations can be quantified, and the uncertainties of the multiplication factor and power distributions for the core simulations can be quantified. As the numerical results presented, the application of NECP-COLEUS to perform sensitivity and uncertainty analysis for the eigenvalue and few-group constants of the lattice calculations, NECP-SUNDEW to perform sensitivity and uncertainty analysis for the eigenvalues and atomic densities with depletions of the burnup calculations and NECP-UNICORN to perform uncertainty analysis for the multiplication factor and power distributions to the steady-stated BEAVRS of the core simulations have been shown and analyzed in this paper.*

I. INTRODUCTION

Sensitivity and Uncertainty (S&U) analysis plays a very important role in the core design and safety analysis for the nuclear reactors, with the increasing demand for the best estimate predictions to be provided with their confidence. In recent years, the reactor physics community has paid much attention on the S&U analysis for the reactor-physics calculations. The Nuclear Engineering Computational Physics (NECP) Laboratory at Xi'an Jiaotong University (XJTU) has been studying on this topic since 2011. Both the widely-applied deterministic method and the statistical sampling method have been applied at XJTU to propagate the nuclear-data uncertainties to the important responses of the reactor-physics calculations, and corresponding code programs have been developed. With the application of the Generalized Perturbation Theory (GPT), the NECP-COLEUS code for the lattice calculations and the NECP-SUNDEW for the burnup calculations have been developed. Applying the statistical sampling method (SSM), the NECP-UNICORN code has been developed for the reactor-physics calculations based on the "two-step" scheme. For NECP-COLUES, the uncertainties of the important responses for the lattice calculations, including the eigenvalue and few-group constants can be quantified; for NECP-SUNDEW, the uncertainties of the important responses of the burnup calculations, including the eigenvalues and atomic densities with depletions can be quantified; for NECP-UNICORN, the uncertainties of the important responses for the reactor-physics calculations, including the eigenvalues, kinetic parameters, few-group constants and atomic densities for the lattice calculations and the multiplication factor and power distributions for the core simulations can be quantified. The theories and applications of these home-developed codes for S&U analysis to the reactor-physics calculations will be introduced in this paper.

II. DESCRIPTION OF THE ACTUAL WORK

With the increasing improvements of the methods and computation capability of the computation machines, the accuracy of the reactor-physics calculations has been notably improved. As the most basic input parameters for the reactor-physics calculations, the nuclear data is measured experiment measurements and evaluated by the theory models, hence the nuclear-data uncertainties are existed inherently and included in the evaluated nuclear-data libraries such as ENDFB-VII.1 and JENDL4.0. According to the observations of the previous researches, the nuclear-data uncertainties have been proved to be one of the most significant uncertainty sources for the reactor-physics calculations and have received the increasing attentions [1].

In this context, the UAM ("Uncertainty Analysis in Modeling") expert group has been organized by the OECD/NEA to establish the benchmarks for the uncertainty analysis in the best-estimate modeling of the coupled multi-physics and multi-scale LWR system, and the propagation of the nuclear-data uncertainties to the important responses of the reactor-physics calculations has received the most focus.

In order to propagate the nuclear-data uncertainties to the significant responses of the reactor-physics calculations, two categories of methodologies have been widely applied: the deterministic method and the statistical sampling method. For the deterministic method, the sensitivity analysis is implemented firstly to obtain the relative sensitivity coefficients of the target or interested responses with respect to the analyzed isotopes and cross sections, with which the relative uncertainties of corresponding responses can be quantified based on the "sandwich rule" combining with the nuclear-data uncertainties. The perturbation theory (PT) or the generalized perturbation theory (GPT) [2] and the direct numerical perturbation method (DNPM) can be used to obtain the relative sensitivity coefficients. For the statistical sampling method (SSM), the nuclear-data samples are generated based on the nuclear-data uncertainties, with which the samples of the interested responses can be obtained by executing the reactor-physics calculations using corresponding nuclear-data samples. The response uncertainties can be quantified based on the response samples using the statistics calculation.

For the PT or GPT based method to perform the S&U analysis, it has the advantage of high efficiency as only one forward and one adjoint neutron-transport calculations are required. However, the notable disadvantages of the PT or GPT based method include the first-order approximation to the uncertainty results and extra efforts in establishment of the perturbation models for different responses. While for the SSM to perform the uncertainty analysis, the notable advantages include no approximation to the uncertainty results and no extra efforts to different responses, with the disadvantage of larger computation cost.

Based on the advantages of the PT or GPT based method and SSM, both methods have been applied in NECP Lab. at XJTU to perform the sensitivity and uncertainty analysis for the reactor-physics calculations. Applying GPT, the code named NECP-COLEUS [3] to perform the S&U analysis for the lattice calculation and NECP-SUNDEW [4] to perform the S&U analysis for the burnup calculation have been developed; applying SSM, the code named NECP-UNICORN [5,6] has been developed to perform uncertainty analysis for the lattice calculations and the core simulations based on the "two-step" scheme. In this paper, the theories of GPT and SSM to the S&U analysis for the reactor-physics calculations have been introduced firstly. As applications, the NECP-COLEUS code applied to the S&U analysis for the eigenvalue and few-group constants of the lattice calculation, NECP-SUNDEW applied to the S&U analysis for the eigenvalues and atomic densities with depletions for the burnup calculations, and NECP-UNICORN applied to the steady-state core simulations of the BEAVRS benchmark problem have been introduced and analyzed.

1. The Deterministic Method for the Sensitivity and Uncertainty Analysis

Sensitivity analysis based on GPT has been proved to be efficient, especially for the case that the number of input parameters far more than the number of the responses. For the calculations of the relative sensitivity coefficients by GPT, the perturbation models should be established for different responses based on corresponding response models. Both the forward and adjoint calculations are required for the sensitivity analysis. In this section, the theories and methods of GPT applied in NECP-COLEUS and NECP-SUNDEW are introduced briefly, with the detailed explanations can be found in our previous works [3, 8].

GPT for the lattice calculation

For the lattice calculations, the homogenized few-group constants of the lattices or assemblies are the important responses, and it can be calculated by the multigroup macroscopic cross sections weighted with the neutron flux characterized as shown in Eq. (1):

$$\bar{\Sigma}_{x,h} = \frac{\left\langle \Sigma_x \boldsymbol{\Phi} \right\rangle}{\left\langle \boldsymbol{\Phi} \right\rangle} \tag{1}$$

where x represents the cross-section type, including the total, absorption, scattering and so on; h is the group index of the homogenized cross sections. The generalized adjoint format according to GPT can be characterized as shown in Eq. (2):

$$\boldsymbol{M}^* \boldsymbol{\Gamma}^* = \frac{\Sigma_x}{\left\langle \Sigma_x \boldsymbol{\Phi} \right\rangle} - \frac{1}{\left\langle \boldsymbol{\Phi} \right\rangle} \tag{2}$$

where $\boldsymbol{M}^*$ is the adjoint operator of the transport operator; $\boldsymbol{\Gamma}^*$ is the generalized adjoint flux. With the forward and adjoint flux $\boldsymbol{\Phi}$ and $\boldsymbol{\Gamma}^*$, the relative sensitivity coefficients of the homogenized few-group constants with respect to the multigroup cross sections can be calculated as shown in Eq. (3):

$$S_{R,\sigma} = \frac{\mathrm{d}R/R}{\mathrm{d}\sigma/\sigma} = \sigma \frac{\left\langle \left(\mathrm{d}\Sigma_x / \mathrm{d}\sigma\right) \boldsymbol{\Phi} \right\rangle}{\left\langle \Sigma_x \boldsymbol{\Phi} \right\rangle} - \sigma \left\langle \boldsymbol{\Gamma}^* \frac{\mathrm{d}\boldsymbol{M}}{\mathrm{d}\sigma} \boldsymbol{\Phi} \right\rangle \tag{3}$$

where $\boldsymbol{M}$ is the transport operator; σ is the specific multi-group cross section; $\boldsymbol{R}$ represents the interested response.

The NECP-COLEUS code has been developed based on our home-developed lattice code Bamboo-Lattice, with the modular MOC for the neutron-transport calculation and the subgroup method for the resonance self-shielding calculations. For the researches of the sensitivity and uncertainty analysis to the LWRs, the explicit and implicit

effects of the multigroup cross sections on the responses should be taken into account. The explicit effect is defined as the direct effects of the effective self-shielding cross sections on the responses through the neutron-transport calculations; while the implicit effect is defined as the indirect effects of the multigroup cross sections on the effective ones through the self-shielding calculations and hence on the responses of the neutron-transport calculations. In NECP-COLEUS, the total effects, including the implicit and explicit ones of the multigroup cross sections on the responses can be quantified. In order to consider the implicit effects in NECP-COLEUS, corresponding derivation based on the subgroup method for the resonance self-shielding calculations has been done and applied. It should be noted that the consideration of the implicit effects based on the subgroup method stepping from the continuous-energy cross sections is innovative and firstly completed in NECP Lab. at XJTU. The implicit relative sensitivity coefficients based on the subgroup method for the resonance self-shielding calculations can be quantified as shown in Eq. (4):

$$S_{\sigma_{x,g},\alpha} = \frac{\sum_{i=1,I} \sigma_{x,g,i} S_{\sigma_{x,g,i},\alpha} \phi_{g,i}}{\sum_{i=1,I} \sigma_{x,g,i} \phi_{g,i}} + \sum_{i=1,I} \int_V \int_{\Omega} \Gamma^*_{x,g,i} \left(Q_{g,i} S_{Q_{g,i},\alpha} - \alpha \frac{\mathrm{d}\boldsymbol{L}}{\mathrm{d}\alpha} \phi_{g,i} \right) \mathrm{d}\boldsymbol{\Omega} \mathrm{d}V \quad (4)$$

where $S_{\sigma_{x,g,i},\alpha}$ is the relative sensitivity coefficient of the subgroup cross sections with respect to the continuous-energy or point-wise ones; $S_{Q_{g,i},\alpha}$ is the relative sensitivity coefficient of the source term with respect to the continuous-energy cross sections; Γ^* is the corresponding generalized subgroup adjoint flux. With the implicit and explicit relative sensitivity coefficients, the total relative sensitivity coefficients of the responses with respect to the multigroup cross sections can be determined. More detailed theory and methods applied for quantifying the explicit relative sensitivity coefficients can be found in our previous work [3].

GPT for the burnup calculation

For the burnup calculation, the responses are generally time-dependent, and hence the time effects should be considered in the process of performing the sensitivity analysis to the burnup calculations. The relative sensitivity coefficients of the responses of the burnup calculation within the depletion period from t_0 (the beginning time of one depletion step) to t_f (the ending time of one depletion step) can be characterized as shown in Eq. (5):

$$S_{R,\sigma} = \int_{t_0}^{t_f} \frac{\mathrm{d}R}{R} \Big/ \frac{\mathrm{d}\sigma}{\sigma} \mathrm{d}t \quad (5)$$

In the burnup calculation, the interested responses $\boldsymbol{R}$, including the eigenvalue (k_∞) and nuclide number density ($\boldsymbol{N}$), are the function of the cross sections ($\boldsymbol{\sigma}$), nuclide number density ($\boldsymbol{N}$), flux ($\boldsymbol{\Phi}$) and adjoint flux ($\boldsymbol{\Phi}^*$), which can be simply characterized as shown in Eq. (6):

$$R = f(\sigma, \mathbf{N}, \mathbf{\Phi}, \mathbf{\Phi}^*) \quad (6)$$

The relative sensitivity coefficients of the responses with respective to the multigroup cross sections can be calculated as shown in Eq. (7):

$$S_{R,\sigma} = \frac{\sigma}{R} \int_{t_0}^{t_f} \left(\frac{\partial R}{\partial \sigma} + \frac{\partial R}{\partial \mathbf{N}} \frac{\mathrm{d}\mathbf{N}}{\mathrm{d}\sigma} + \frac{\partial R}{\partial \mathbf{\Phi}} \frac{\mathrm{d}\mathbf{\Phi}}{\mathrm{d}\sigma} + \frac{\partial R}{\partial \mathbf{\Phi}^*} \frac{\mathrm{d}\mathbf{\Phi}^*}{\mathrm{d}\sigma} \right) \mathrm{d}t \quad (7)$$

With the traditional prediction-correction scheme for the burnup calculation, the flux and adjoint flux within each depletion step are assumed to be constant. Therefore, the Eq. (7) can be re-characterized as Eq. (8):

$$S_{R,\sigma} = \frac{\sigma}{R} \left(\int_{t_0}^{t_f} \frac{\partial R}{\partial \sigma} \mathrm{d}t + \int_{t_0}^{t_f} \frac{\partial R}{\partial \mathbf{N}} \frac{\mathrm{d}\mathbf{N}}{\mathrm{d}\sigma} \mathrm{d}t + \sum_{i=0}^{I-1} \frac{\mathrm{d}\mathbf{\Phi}_i}{\mathrm{d}\sigma} \int_{t_i}^{t_{i+1}} \frac{\partial R}{\partial \mathbf{\Phi}_i} \mathrm{d}t + \sum_{i=0}^{I-1} \frac{\mathrm{d}\mathbf{\Gamma}^*_i}{\mathrm{d}\sigma} \int_{t_i}^{t_{i+1}} \frac{\partial R}{\partial \mathbf{\Gamma}^*_i} \mathrm{d}t + \frac{\partial R}{\partial \mathbf{N}_I} \frac{\mathrm{d}\mathbf{N}_I}{\mathrm{d}\sigma} + \frac{\partial R}{\partial \mathbf{\Phi}_I} \frac{\mathrm{d}\mathbf{\Phi}_I}{\mathrm{d}\sigma} + \frac{\partial R}{\partial \mathbf{\Phi}^*_I} \frac{\mathrm{d}\mathbf{\Phi}^*_I}{\mathrm{d}\sigma} \right) \quad (8)$$

where i is the index of one specific depletion step; I is the total number of the depletion steps; t_i and t_{i+1} are the beginning and ending time of the ith depletion step. In order to quantify the relative sensitive coefficients as shown in Eq. (8), four extra equations [7] are required and should be solved as shown in Eq. (9)~(12):

$$\frac{d\mathbf{N}_i(t)}{dt} = \mathbf{M}_i \mathbf{N}_i(t) \quad (9)$$

$$\mathbf{M}_i \mathbf{\Phi}_i = 0 \quad (10)$$

$$\mathbf{M}^*_i \mathbf{\Gamma}^*_i = 0 \quad (11)$$

$$P_i = \int_V \sum_k \kappa^k \sigma^k_f N^k_i \mathbf{\Phi}_i dV \quad (12)$$

where Eq. (9) is the depletion equation, Eq. (10) and (11) stand for the neutron-transport equation with the forward and adjoint format respectively, Eq. (12) is the equation for the power calculation. With these equations, the relative sensitivity coefficients of the important responses with respect to the multigroup cross sections shown in Eq. (8) can be calculated as shown in Eq. (13):

$$S_{R,\sigma} = \frac{\sigma}{R} \left(\int_{t_0}^{t_f} \frac{\partial R}{\partial \sigma} \mathrm{d}t + \sum_{i=0}^{I-1} \int_{t_i}^{t_{i+1}} \mathbf{N}^* \frac{\partial \mathbf{M}_i}{\partial \sigma} \mathbf{N} \mathrm{d}t + \sum_{i=0}^{I} \mathbf{\Gamma}^*_i \frac{\partial \mathbf{B}_i}{\partial \sigma} \mathbf{\Phi}_i + \sum_{i=0}^{I} \mathbf{\Gamma}_i \frac{\partial \mathbf{B}^*_i}{\partial \sigma} \mathbf{\Phi}^*_i - \sum_{i=0}^{I} P^*_i \frac{\partial P_i}{\partial \sigma} \right) \quad (13)$$

where $\boldsymbol{N}$, $\boldsymbol{M}$, $\boldsymbol{B}$, $\boldsymbol{B}^*$, $\boldsymbol{\Phi}$, $\boldsymbol{\Phi}^*$, and P can be calculated by solving the forward depletion equation; and the $\boldsymbol{N}^*$, $\boldsymbol{\Gamma}$, $\boldsymbol{\Gamma}^*$ and P^* can be calculated by solving the extra equations shown as Eq. (9)~(12).

The "Sandwich Rule" for Uncertainty Analysis

With the relative sensitivity coefficients provided by the sensitivity analysis, the relative uncertainties of the interested responses of the reactor-physics calculations can

be quantified using the "sandwich rule", which can be characterized as shown in Eq. (14):

$$\frac{\Delta R^2}{R^2} = \mathbf{S}_{R,\sigma}\boldsymbol{\Sigma}_r\mathbf{S}_{R,\sigma}^T \quad (14)$$

where $\boldsymbol{S}_{R,\sigma}$ is the relative sensitivity coefficient of the responses with respect to the multigroup cross sections; $\boldsymbol{\Sigma}_r$ stands for the relative covariance matrices of the multigroup cross sections. The relative covariance matrices of the multigroup cross sections can be generated based on the evaluated nuclear-data files, e.g. ENDF/B-VII.1 and JENDL4.0 using the NJOY code.

2. The Statistical Sampling Method for the Uncertainty Analysis

In this sub-section, the theories and methods of the statistical sampling method for the uncertainty analysis has been introduced briefly, with the detailed introductions are given in our previous works [5, 6].

The theory and method

Using the SSM for the uncertainty analysis, the samples of the input parameters are required and generated firstly. With the relative covariance matrix of the multigroup cross sections, the samples of the relative perturbation factors can be obtained as shown in Eq. (15):

$$\boldsymbol{X}_S = \boldsymbol{\Sigma}_r^{1/2}\boldsymbol{Y}_S + \boldsymbol{1.0} \quad (15)$$

where $\boldsymbol{X}_S$ stands for the samples of the relative perturbation factors and $\boldsymbol{Y}_S$ is the samples of the independent parameters. For the sampling process to the multigroup cross sections, relative perturbations are actually added to the multigroup cross sections. Therefore, corresponding multigroup cross-section perturbation model has been designed and applied in NECP-UNICORN. With $\boldsymbol{X}_S$ and the multigroup cross-section perturbation model, the perturbed or sampled multigroup cross-section libraries can be obtained. The reactor-physics calculations are carried out with the samples of the multigroup microscopic cross-section library, with the corresponding samples of the responses $\boldsymbol{R}_S$ can be obtained. Finally, the covariance matrix of the responses can be determined as shown in Eq. (16):

$$\boldsymbol{\Sigma}_{\boldsymbol{R},i,j} = \frac{1}{nS-1}\sum_{n=1}^{nS}(R_{i,n}-R_{i,0})(R_{j,n}-R_{j,0}) \quad (16)$$

where nS is the size of the samples; $\boldsymbol{\Sigma}_{\boldsymbol{R}}$ represents the covariance matrix of responses with the size of $nR \times nR$; $\boldsymbol{\Sigma}_{\boldsymbol{R},i,j}$ is the covariance for the *ith* and *jth* response (i,j =1,2,…,nR); $R_{i,n}$ (or $R_{j,n}$) and $R_{i,0}$ (or $R_{j,0}$) stand for the *nth* sample value and expectation value for the *ith* (or *jth*) response R_i (or R_j), which can be characterized as shown in Eq. (17).

$$R_{i,0} = \frac{1}{nS}\sum_{n=1}^{nS}R_{i,n} \quad (17)$$

The multigroup cross-section perturbation model

The sampling process is actually the process of perturbing the multigroup cross sections to the required values, hence the multigroup cross-section perturbation model has been established and applied in the NECP-UNICORN code.

The multigroup cross-section library is essential for solving the neutron-transport equation with the deterministic method. With the energy- and temperature-dependent pointwise cross sections, the multigroup cross sections with specific format can be converted into, using the weighting flux $\phi(E,\sigma_0)$ as shown in Eq. (18):

$$\sigma_{x,g}(T,\sigma_0) = \frac{\int_{\Delta E_g}\sigma_x(E,T)\phi(E,\sigma_0)dE}{\int_{\Delta E_g}\phi(E,\sigma_0)dE} \quad (18)$$

where T, E and σ_0 represent the temperature, energy and background cross section respectively; $\sigma_x(E,T)$ is the energy- and temperature-dependent pointwise cross section of type x, and $\phi(E,\sigma_0)$ represents the weighting flux at condition of σ_0. It should be noted that for the non-resonance cross sections and resonance cross sections within non-resonance groups, the σ_0 can be considered to be infinite, and the weighting flux $\phi(E,\sigma_0)$ is only the function of energy. While for the resonance cross sections within resonance energy range, the weighting flux is dependent on both energy and dilution cross sections.

Since the multigroup cross sections are converted from the pointwise cross sections with application of Eq. (18), the cross-section perturbations added to the multigroup cross sections should be consistent with the identical perturbations propagated from the pointwise cross sections to the multigroup ones. Therefore, in the multigroup cross-section perturbation model, the relative perturbations for the *gth* group of type x is performed by adding the uniform relative perturbations to the pointwise cross section within the energy range of the *gth* group as shown in Eq. (19):

$$\sigma_x'(E,T) = (1+\delta_{x,g})\sigma_x(E,T) \quad E_{g-1} \le E \le E_g \quad (19)$$

where $E_{g\text{-}1}$ and E_g stand for the lower and upper energy boundaries for the *gth* group; $\delta_{x,g}$ represents the relative perturbation uniformly added to the pointwise cross section of type x within energy range of *gth* group; $\sigma_x'(E,T)$ represents the perturbed pointwise cross section of type x.

For the cross sections without resonance, the weighting flux is selected or input by users and independent of the point-wise cross sections. Therefore, the perturbation propagations from the point-wise cross sections to these multigroup ones are linear and can be characterized as shown in Eq. (20).

$$\sigma_{x,g}'(T) = \frac{\int_{\Delta E_g}\sigma_x'(E,T)\phi(E)dE}{\int_{\Delta E_g}\phi(E)dE} = (1+\delta_{x,g})\sigma_{x,g}(T) \quad (20)$$

However, for the resonant cross sections, the perturbation propagations are non-linear. Because the weighting flux within resonance-energy regions would be

perturbed at the same time due to perturbations to the point-wise cross sections. Therefore, strict derivation should be performed to determine the correct propagations of perturbations from the point-wise cross sections to the multigroup ones. With the *NR* approximation to the weighting flux within the resonance energy regions, the perturbed resonant cross sections can be characterized as Eq. (21):

$$\sigma'_{x,g}(T,\sigma_0)=\frac{\int_{\Delta E_g}\sigma'_x(E,T)\phi'(E,\sigma_0)dE}{\int_{\Delta E_g}\phi'(E,\sigma_0)dE}=(1+\delta_{x,g})\sigma_{x,g}(T,\sigma'_0) \quad (21)$$

where σ'_0 stands for the perturbed background cross sections due to perturbations of point-wise cross sections which can be expressed as shown in Eq. (22):

$$\sigma'_0=\frac{\sigma_0}{1+\delta_{t,g}} \quad (22)$$

where $\delta_{t,g}$ presents the relative perturbation of total cross section due to the relative perturbations $\delta_{x,g}$ of type *x*. After the perturbations of the multigroup cross sections, corresponding consistent rules are used to keep the cross sections balance and consistent.

As the NR approximation has been applied for the weighting flux within the resonance energies, the ultrafine-group cross-section perturbation model has been proposed in NECP Lab. at XJTU. The actual perturbations are applied to the ultrafine-group cross-section library and the reconstructions of the resonance cross sections are performed by solving the neutron slowing-down equation.

After the relative perturbation adds into the ultrafine-group cross sections within the resonance energy, corresponding perturbed weighting flux can be quantified by solving the neutron slowing-down equation as shown in Eq. (23).

$$\Sigma_{t,i}(T)\phi'_i(\sigma_0)=\sum_{i'}\Sigma_{s,i'\to i}(T)\phi'_{i'}(\sigma_0) \quad (23)$$

where the subscript *i* and *i*' stand for the ultrafine groups; σ_0 is the dilution cross sections and can be set to expected value by varying the atom density ratio of non-resonant nuclide to the resonant one. With the perturbed weighting flux, corresponding perturbed multigroup cross section of type *x* for the *gth* group can be converted as shown in Eq. (24).

$$\sigma'_{x,g}(T,\sigma_0)=\frac{\sum_{i\in g}\overline{\sigma}'_{x,i}(T)\phi'_i(\sigma_0)}{\sum_{i\in g}\phi'_i(\sigma_0)} \quad (24)$$

Where $\overline{\sigma}'_{x,i}$ is the perturbed ultrafine-group cross section, *i* and *g* stand for the group number of ultrafine-group and multigroup energy structure respectively. From our previous research [9], it can be found that the NR approximation overestimates the relative sensitivity coefficients and the corresponding uncertainty results for the LWR pin-cells, and the effects of the NR approximation are significant for $\sigma_{(n,\gamma)}$ and $\sigma_{(n,elas)}$ of ^{238}U.

III. RESULTS AND ANALYSIS

With the brief introductions to the theories and methods applied in NECP Lab. at XJTU, corresponding codes for the sensitivity and uncertainty analysis of the reactor-physics calculations have been developed. These codes have the capabilities of quantifying the relative sensitivity coefficients and uncertainties of the important responses for the reactor-physics calculations, including the lattice calculations, burnup calculations and core simulations. The most recent applications and researches for the sensitivity and uncertainty of the reactor-physics calculations using our home-developed codes NECP-COLEUS, NECP-SUNDEW and NECP-UNICORN will be shown in this section.

1. Application and Researches by NECP-COLEUS

The NECP-COLEUS code has the capability of sensitivity and uncertainty analysis to the lattice calculations, quantifying the relative sensitivity coefficients and uncertainties for the eigenvalue and few-group constants. As application of NECP-COLEUS, the UAM pin-cell benchmark PB-2 pin-cell has been analyzed, with the analyzed responses to be the eigenvalue and two-group constants. In order to study the implicit effects of the LWRs, the comparisons of the explicit and total (sum of the explicit and implicit effects) relative sensitivity coefficients for the eigenvalue and two-group constants with respect to ^{238}U-σ_γ are shown in Fig. 1. As the implicit effects are due to the resonant cross sections within the resonance groups, only the comparisons are focused on and shown within the resonance groups, e.g. 15th ~27th group for the 69-group energy-group structure. In Fig.1, the $\Sigma_{c,1}$ stands for the capture constant of the fast group; $\nu\Sigma_{f,1}$ is the neutron yield constant of the fast group, and the $\Sigma_{s,1\text{-}1}$ presents the scattering constant from the fast group to the fast group.

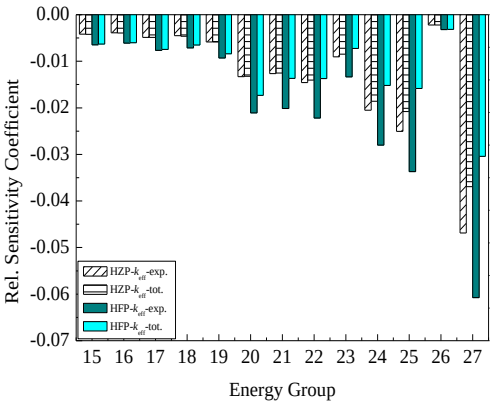

(a). For k_∞

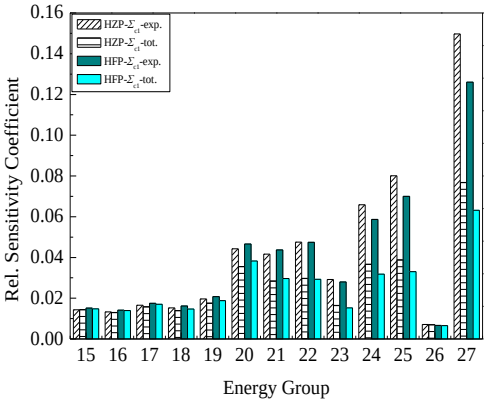

(b). For $\Sigma_{c,1}$

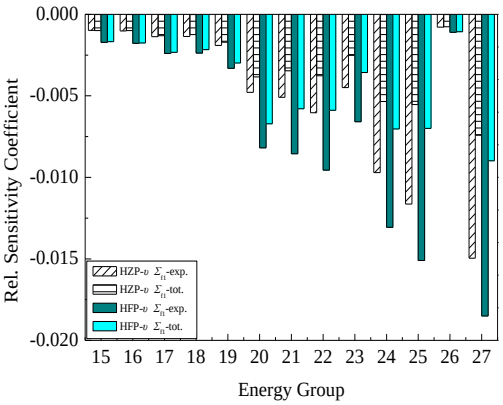

(c). For $\nu\Sigma_{f,1}$

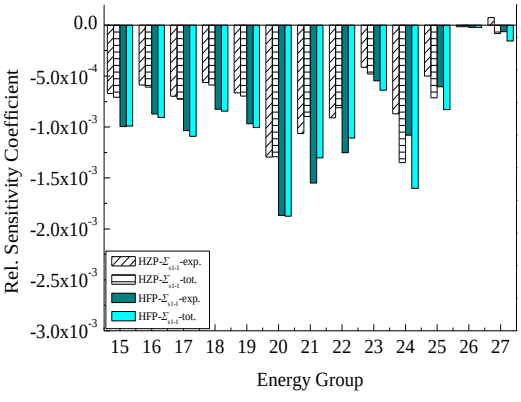

(d). For $\Sigma_{s,1-1}$

Fig.1 The comparison of relative sensitivity coefficients of ^{238}U-σ_γ

From the numerical comparisons, it can be found that the differences between the explicit and total relative sensitivity coefficients are notable, which implies that the implicit effects of the multigroup cross section on the responses are significant for the LWRs, hence should be taken into account.

With consideration of the implicit effects, the relative uncertainties of the eigenvalue and two-group constant of the PB-2 pin-cell introduced by the nuclear-data uncertainties at the Hot Zero Power (HZP) and Hot Full Power (HFP) conditions are compared and shown in Fig. 2. The nuclear-data uncertainties are generated based on ENDF/B-VII.1 using the NJOY code. It can be numerically observed that for the eigenvalue, the relative uncertainty is about 4.8‰ at HZP and 5.9‰ at HFP; for the two-group constants, the relative uncertainties can up to be 1.4% for the $\Sigma_{c,1}$. Moreover, the relative uncertainties of the responses at HFP are larger than those at HZP.

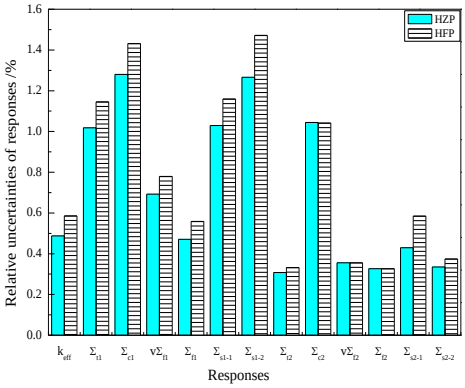

Fig.2 The relative uncertainties of responses at HZP and HFP

From the numerical results obtained by applying NECP-COLEUS to the sensitivity and uncertainty analysis to the lattice calculations, two aspects of conclusions can be obtained. Firstly, the implicit effects are significant for the LWRs and should be considered; secondly, the relative uncertainties of the few-group constants introduced by the nuclear-data uncertainties are notable.

2. Application and Researches by NECP-SUNDEW

The NECP-SUNDEW code has the capability of sensitivity and uncertainty analysis for the burnup calculations, quantifying the relative sensitivity coefficients and relative uncertainties of the eigenvalue and atomic densities with depletions. As application of NECP-SUNDEW, the UAM burnup benchmark TMI-1 pin-cell has been analyzed. For the application, the nuclear-data uncertainties are generated based on both ENDF/B-VII.1 and JENDL4.0 using the NJOY code. Relative uncertainties of the eigenvalues and atomic densities with depletions have been quantified and compared as shown in Fig. 3, with detailed contributions of the important isotopes and cross sections to the total uncertainty given.

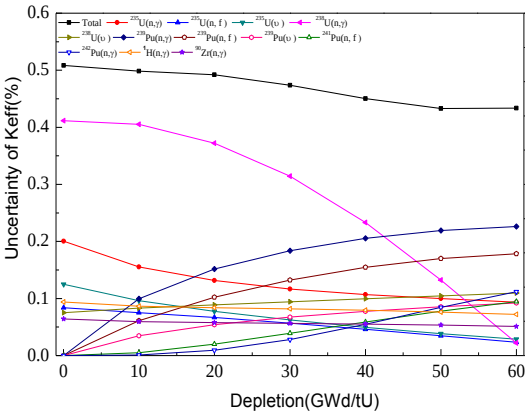

(a). By ENDF/B-VII.1

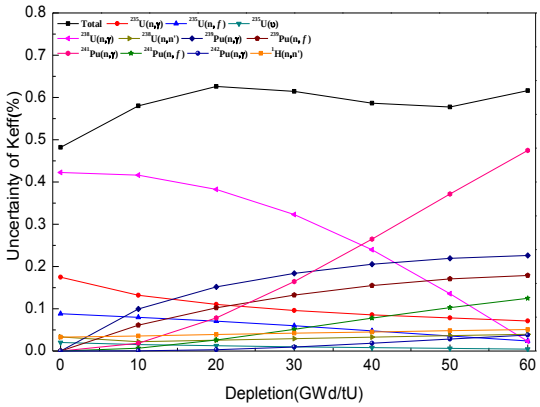

(b). By JENDL4.0

Fig.3 The relative uncertainties of k_∞ by ENDF/B-VII.1 and JENDL4.0

From the numerical results and comparisons, it can be observed that nuclear-data uncertainties contained in ENDF/B-VII.1 introduce larger uncertainties to k_∞ than those contained in JENDL4.0. For ENDF/B-VII.1, the relative uncertainties of k_∞ are 500 pcm at the Beginning Of Cycle (BOC) and 430 pcm at the Ending Of Cycle (EOC); while for the JENDL4.0, the values are 480 pcm at BOC and 620 pcm at EOC. Moreover, the relative uncertainties of the eigenvalue vary notably with the depletions.

The relative uncertainties of the atomic densities of the important isotopes during depletions are shown in Table 1. As the nuclear-data uncertainties of the main fission products are not available in JENDL4.0, the uncertainties on the main fission products can't be quantified in this paper.

Table 1. Relative uncertainties / % of the nuclide number densities

Isotopes	10GWd/tU		30 GWd/tU		50 GWd/tU	
	ENDF/B-VII.1	JENDL 4.0	ENDF /B-VII.1	JENDL 4.0	ENDF /B-VII.1	JENDL 4.0
Ag-109	1.20	--	1.37	--	1.78	--
Xe-131	0.93	--	3.00	--	5.16	--
Cs-134	3.11	--	3.13	--	3.25	--
Nd-143	0.29	--	0.94	--	1.69	--
Nd-145	0.28	--	0.95	--	1.74	--
Sm-149	4.90	--	5.02	--	5.32	--
Sm-151	4.71	--	5.73	--	6.07	--
Eu-151	4.17	--	5.86	--	6.62	--
Eu-155	24.46	--	27.13	--	28.06	--
Gd-154	4.97	--	4.43	--	3.75	--
Gd-155	23.96	--	25.84	--	25.28	--
Gd-156	0.87	--	1.96	--	3.33	--
Gd-157	4.19	--	4.47	--	4.87	--
U-234	0.13	0.57	0.43	1.81	0.80	3.27
U-235	0.08	0.07	0.48	0.55	1.41	1.88
U-236	1.39	1.14	1.36	1.09	1.31	1.06
U-237	1.93	1.72	2.67	2.31	2.83	2.47
U-238	0.01	0.01	0.03	0.03	0.05	0.05
Np-237	1.47	1.33	2.49	2.16	3.05	2.60
Pu-238	4.39	3.70	4.05	4.30	4.04	5.54
Pu-239	1.67	1.72	2.09	2.27	2.65	3.11
Pu-240	1.92	7.97	2.14	12.72	2.44	15.84
Pu-241	1.95	16.67	1.82	9.88	2.21	8.08
Pu-242	2.86	20.53	3.01	13.90	4.01	11.30
Am-241	2.14	18.23	2.72	11.80	4.08	10.74
Am-243	11.45	22.08	10.34	15.72	9.05	12.67
Cm-244	12.09	23.51	11.12	17.54	9.95	14.13

From the results shown in Table 1, it can be observed that the relative uncertainties of most heavy isotopes induced by the nuclear-data uncertainties contained in JENDL4.0 are larger than those introduced by ENDF/B-VII.1, especially to the heavy isotopes heavier than ^{239}Pu. This observation is due to the larger nuclear-data uncertainties contained in JENDL4.0 than those contained in ENDF/B-VII.1.

As conclusion of applying NECP-SUNDEW to the sensitivity and uncertainty analysis for the burnup calculation of the TMI-1 pin-cell, two observations can be obtained. Firstly, the relative uncertainties of the eigenvalues and atomic densities vary notably with the depletions; secondly, different sources of the nuclear-data uncertainties result in different uncertainties to the important responses with deeper depletions: for the eigenvalue, the relative uncertainties introduced by the nuclear-data uncertainties contained in JENDL4.0 are larger than those contained in ENDF/VII.1; for the atomic densities, the nuclear-data uncertainties contained in JENDL4.0 introduce notably larger uncertainties to some isotopes, including ^{241,242}Pu, ^{241,243}Am and ^{244}Cm.

3. Uncertainty Analysis for BEAVRS by NECP-UNICORN

The NECP-UNICORN code has the capability of sensitivity and uncertainty analysis for the reactor-physics calculations, including the lattice calculations, burnup calculations and core simulations. Any kinds of interested responses of the lattice calculations, burnup calculations and core simulations can be analyzed. As application of NECP-UNICORN, the uncertainty analysis has been performed to the BEAVRS benchmark problem at the HZP conditions based on the "two-step" scheme, propagating the nuclear-data uncertainties from the multigroup cross section to the eigenvalue and few-group constants of the lattice calculations and then to the multiplication factor and power distributions of the core simulation. The nuclear-data uncertainties contained in ENDF/B-VII.1 are generated and applied in the uncertainty analysis in this paper.

The relative uncertainties of the eigenvalue and two-group constants for the 9 different assemblies of the

BEAVRS benchmark are shown in Table 2. In Table 2, 31000, 31006, 31015, 31016, 31020, 24000, 24012, 24016 and 16000, represent the fuel assemblies 3.1% with 0 BA, 3.1% with 6 BA, 3.1% with 15 BA, 3.1% with 16 BA, 3.1% with 20 BA, 2.4% with 0 BA, 2.4% with 12 BA, 2.4% with 16 BA and 1.6% with 0 BA, where the percentage stands for the enrichment of ^{235}U and BA represents the burnable absorber. The results in Table 2 consist of two parts: the expectation values of the relative uncertainties and corresponding statistical errors.

From the numerical results, it can be observed that the relative uncertainties for the eigenvalues of the fuel assemblies vary from 5.0‰ to 5.7‰; and the largest relative uncertainties of the two-group constants can up to be 1.65% for D_1, the fast-group diffusion coefficient. Moreover, the relative uncertainties of the fast-group constants are larger than those of the thermal group.

The relative uncertainty of the multiplication factor of the core simulation is 5.1‰, with the same magnitude as the uncertainties encountered in the eigenvalues of the fuel assemblies. The relative uncertainties of the power distributions of the core are shown in Fig. 4.

0.70	0.79	0.80	0.96	0.87	0.97	0.95	1.02
4.27	3.98	3.47	2.68	1.91	0.70	0.66	1.69
0.79	0.76	0.92	0.86	1.00	0.90	1.14	1.07
3.98	3.82	3.21	2.60	1.66	0.62	0.89	1.79
0.80	0.92	0.86	1.01	0.91	1.01	0.95	0.96
3.47	3.21	2.80	2.02	1.27	0.16	0.99	1.87
0.96	0.86	1.01	0.95	1.10	1.03	1.19	0.78
2.68	2.60	2.02	1.30	0.28	0.59	1.63	1.93
0.87	1.00	0.91	1.10	1.44	1.21	1.26	
1.91	1.66	1.27	0.28	0.83	1.55	2.23	
0.97	0.90	1.01	1.03	1.21	1.28	0.94	
0.70	0.62	0.16	0.59	1.55	2.28	2.52	
0.95	1.14	0.95	1.19	1.26	0.94		
0.66	0.89	0.99	1.63	2.23	2.52		
1.02	1.07	0.96	0.78			Assembly Power	
1.69	1.79	1.87	1.93			Rel. Unc./%	

Fig.4 The radial power distributions and relative uncertainties

Table 2. Relative uncertainties / % of the eigenvalue and two-group constants

	16000/%	24000/%	24012/%	24016/%	31000/%	31006/%	31015/%	31016/%	31020/%
k_∞	0.57±0.02	0.52±0.02	0.52±0.02	0.52±0.02	0.50±0.02	0.50±0.02	0.50±0.02	0.50±0.02	0.50±0.02
D_1	1.65±0.11	1.62±0.11	1.64±0.11	1.65±0.11	1.60±0.11	1.61±0.11	1.62±0.11	1.63±0.11	1.63±0.11
D_2	0.37±0.02	0.37±0.02	0.37±0.02	0.37±0.02	0.37±0.02	0.37±0.02	0.37±0.02	0.37±0.02	0.37±0.02
$\Sigma_{a,1}$	1.02±0.06	0.96±0.05	0.96±0.05	0.96±0.05	0.92±0.05	0.92±0.05	0.92±0.05	0.93±0.05	0.93±0.05
$\Sigma_{a,2}$	0.44±0.02	0.39±0.01	0.34±0.01	0.33±0.01	0.36±0.01	0.34±0.01	0.32±0.01	0.31±0.01	0.30±0.01
$\nu\Sigma_{f,1}$	1.03±0.05	0.76±0.04	0.76±0.04	0.75±0.04	0.64±0.03	0.63±0.03	0.63±0.03	0.63±0.03	0.62±0.03
$\nu\Sigma_{f,2}$	0.39±0.01	0.38±0.01	0.38±0.01	0.38±0.01	0.38±0.01	0.38±0.01	0.38±0.01	0.38±0.01	0.38±0.01
$\Sigma_{s,1,1}$	1.01±0.06	1.01±0.06	1.01±0.06	1.02±0.06	1.00±0.06	1.00±0.06	1.01±0.06	1.01±0.06	1.01±0.06
$\Sigma_{s,1,2}$	1.18±0.06	1.11±0.06	1.18±0.06	1.21±0.06	1.08±0.06	1.11±0.06	1.16±0.06	1.16±0.06	1.18±0.06
$\Sigma_{s,2,1}$	0.57±0.03	0.55±0.03	0.53±0.03	0.53±0.03	0.54±0.03	0.54±0.03	0.52±0.03	0.52±0.03	0.52±0.03
$\Sigma_{s,2,2}$	0.35±0.02	0.35±0.02	0.36±0.02	0.36±0.02	0.35±0.02	0.36±0.02	0.36±0.02	0.36±0.02	0.36±0.02

It can be observed form the results in Fig. 4 that the maximum relative uncertainty of the 2D radial power distributions is 4.27%, occurred in the middle of the reactor with lower assembly power. The RMS of the relative uncertainties of the 2D radial power distributions is 2.08%.

As conclusions of applying NECP-UNICORN to the uncertainty analysis for the BEAVRS benchmark at HZP, two aspects of observations can be obtained. Firstly, the relative uncertainty of the multiplication factor for the core simulation has the same magnitude of the eigenvalue of the fuel assemblies for the lattice calculations; secondly, the relative uncertainties of the power distributions introduced by the nuclear-data uncertainties are notable and significant for the reactor-physics calculations.

IV. CONCLUSIONS

In this paper, the most recent researches on the sensitivity and uncertainty analysis for the reactor-physics calculations completed in NECP Lab. at XJTU have been introduced and presented briefly.

The widely applied methods have been utilized to perform the sensitivity and uncertainty analysis for the reactor-physics calculations, and corresponding analysis codes have been developed. Applying the generalized perturbation theory (GPT), the codes named NECP-COLEUS and NECP-SUNDEW have developed for the lattice calculation and burnup calculations respectively; applying the statistical sampling method (SSM), the code named NECP-UNICORN has been developed based on the "two-step" scheme for the reactor-physics calculations. From the view of the theories and applications, for GPT, it has the notable advantage of high efficiency and also the disadvantage that different perturbation modes should be established for different responses and the first-order approximation to the uncertainty results; for SSM, it has the notable advantage that no extra effort is required for different responses and the notable disadvantage of huge-amount computation cost. In order to quantify the relative sensitivity coefficients and corresponding uncertainties of the important responses in the level of lattice calculations, the codes based on GPT are the first choice. While for the

uncertainty propagations to the core simulations and even further to the level of the thermal-hydraulics calculations and safety analysis of the whole reactor, the advantage of SSM would be more and more notable and should be the first choice. Therefore, through our researches on the sensitivity and uncertainty analysis of the reactor-physics calculations, both the GPT and SSM have their advantages and disadvantages, hence capable for different applications.

REFERENCES

1. Ivanov, K., Avramova, M., Kamerow, S., Kodeli, I., Sartori, E., Ivanov, E., Cabellos, O., 2013. Benchmarks for Uncertainty Analysis in Modelling (UAM) for the Design, Operation and Safety Analysis of LWRs. OECD Nuclear Energy Agency, NEA/NSC/ DOC (2013)7.
2. M. Pusa, "Perturbation-Theory-Based Sensitivity and Uncertainty Analysis with CASMO-4," Science and Technology of Nuclear Installations(2012).
3. Y. Liu, L. Cao, H. Wu, et al., Eigenvalue implicit sensitivity and uncertainty analysis with the subgroup resonance-calculation method, Annals of Nuclear Energy, **79**, 18–26(2015).
4. Zu T, Yang C, Cao L, et al. Nuclear data uncertainty propagation analysis for depletion calculation in PWR and FR pin-cells. Annals of Nuclear Energy, 2016, 94:399-408.
5. Wan, C., Cao, L., Wu, H., et al., 2015. Code development for eigenvalue total sensitivity analysis and total uncertainty analysis. Annals of Nuclear Energy 85, 788-797.
6. Zu, T., Wan, C., Cao, L., et al., 2016. Total Uncertainty Analysis for PWR Assembly Based on the Statistical Sampling method. Nuc. Sci. & Eng, 183: 371-386.
7. Takeda T., Umano T., Burn-up sensitivity analysis in a fast breeder reactor –part I: sensitivity calculation method with generalized perturbation theory, Nucl. Sci. Eng., 91, p.l-10(1985).
8. Zu, T., Yang, C., Cao, L., Wu, H., 2016. Nuclear data uncertainty propagation analysis for depletion calculation in PWR and FR pin-cells, Annals of Nuclear Energy 94, 399-408.
9. Wan, C., Cao, L., Wu, H., Shen, W., 2017. Total sensitivity and uncertainty analysis for LWR pin-cells with improved UNICORN code, Annals of Nuclear Energy 99, 301-310.